

# Determination Of The Stress State Developed Within A Non-Cushioned Rail Yoke And The Prediction Of The Theoretical Fatigue Life

Andrew Smyth<sup>1\*</sup>, Jason Reiling<sup>1</sup>, Sean Ely<sup>1</sup>

<sup>1</sup> *Strato Inc., 100 New England Ave., Piscataway, 08854, USA*

E-mail: [asmith@stratoinc.com](mailto:asmith@stratoinc.com), [jreiling@stratoinc.com](mailto:jreiling@stratoinc.com), [sely@stratoinc.com](mailto:sely@stratoinc.com)

**Abstract:** During service, freight railroad coupling systems experience heavy loading due to various train actions. For non-cushioned railcars, the primary tensile component utilized to transfer these forces to the draft system is the yoke. The stress state developed within a yoke was analyzed using both strain gage data and nonlinear finite element methods for both static maximal loads and pseudo-static cyclic loads accounting for the nonlinear material behavior, including plasticity and strain hardening. From the stress profile developed within a yoke the theoretical fatigue life was calculated using various strain life fatigue analysis methods considering both uniaxial and biaxial stress conditions. Using this data, the critical locations were confirmed and a prediction of service failure is presented.

**Index Terms:** yoke, stress analysis, FEA, fatigue

## INTRODUCTION AND PROBLEM DESCRIPTION

**Finite element analysis (FEA)**

**True ultimate tensile strength (UTS)**

**Since the yoke is symmetric about two planes, a quarter symmetry model can be used in the FEA analysis to reduce computation time and to increase the accuracy of the results.**

## STATIC STRESS ANALYSIS

There are two basic types of yoke failure in the field; one being the fracture of the yoke and the other being excessive stretching thus making removal of the yoke from the coupler system difficult. To determine the critical locations on a yoke a theoretical stress analysis was performed in conjunction with a strain gage analysis to develop an understanding of the possible failure zones within both styles of yoke. The static loading conditions used for the analyses were based on the M-205 testing described in the AAR manual (1), including the ultimate tensile test and the permanent set test. For the ultimate tensile

test, each yoke must be able to withstand a maximum tensile load of 900 kips without failure. Before the yoke is loaded to 900 kips, the permanent set test is performed by first loading the yoke to 750 kips and then unloading to 5 kips (original datum value). After unloading, the yoke must have a permanent set no greater than 0.03 inches. While performing these tests in the lab (test set-up shown in **Figure 1**), 3 strain gage rosettes were attached to locations that were deemed critical based on our preliminary FEA simulations. The strain gage locations are shown in **Figure 2** marked with an 'X'.

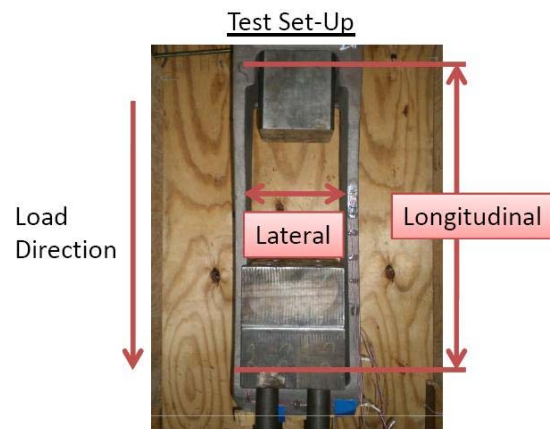


Figure 1: Test Set-Up

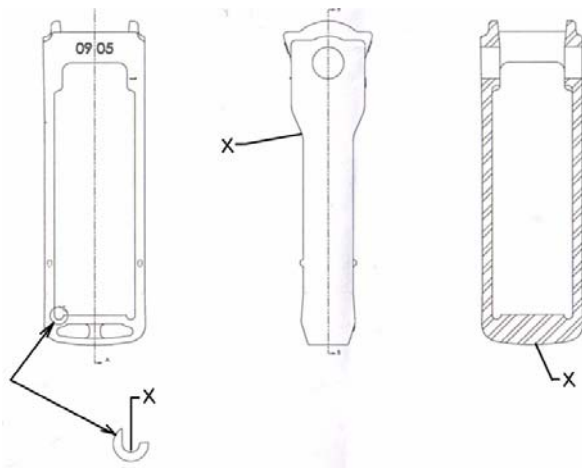


Figure 2: Rosette Locations

To validate our FEA stress results we attempted to correlate both the actual strain gage data with the theoretical FEA results. When performing the testing described in M-205, the ultimate tensile test is performed immediately after the permanent set test. Since the testing is continuous the graphs shown have an abscissa of an arbitrary time. For the comparison, the time is non dimensional as the static FEA analysis only uses time as a loading placeholder; no inertia effects needed to be considered. In addition to the strain gage data obtained, two displacements were measured: longitudinal and lateral, as shown in **Figure 1**.

The longitudinal displacements were measured in the axial direction coinciding with the direction of the load. Since the loading is exclusively tensile it will cause the yoke to stretch, thus producing the positive longitudinal displacement values. This extension of the yoke will cause the straps to

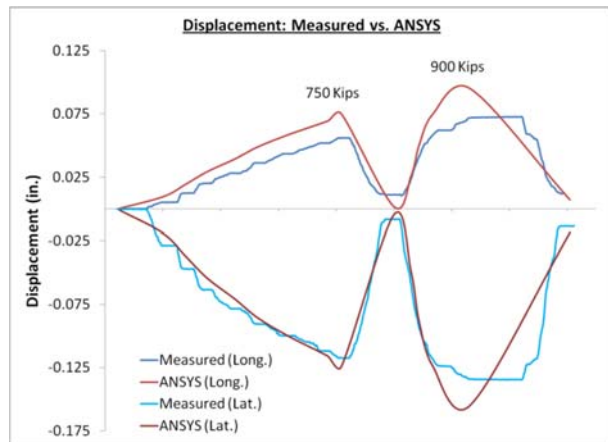


Figure 4: Displacement Correlation

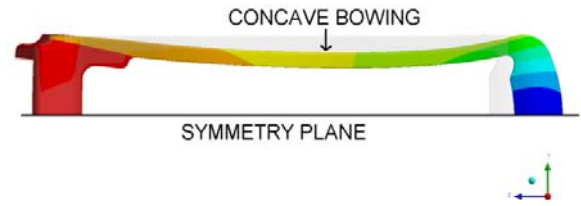


Figure 3: Deformation - 10x Scale

bow inward creating a negative displacement measurement. **Figure 4** plots both displacements versus time for the duration of the entire test. To illustrate the concave nature of the strap under a loading, a 10x scaled contour plot of the displacement is shown in **Figure 3**. This plot displays the nature of deformation that a yoke will experience under a tensile load.

To easily compare the strain gage rosette data to the results obtained from the FEA simulation a conversion was performed to represent the rosette strains as an equivalent strain. For the tensile test, 45 degree rosettes were installed on the three locations shown in **Figure 2**. The strain output from each rosette consists of the three strain measurements corresponding to the three gages located in each rosette. These three strains are then converted into the three in-plane strains  $\epsilon_x$ ,  $\epsilon_y$  and  $\epsilon_{xy}$  as shown in (2). These directional strains, along with the out-of-plane strain  $\epsilon_z$ , calculated using Hooke's Law as shown in (3), are then transformed into the principal coordinate system using (1) thus outputting the three principal strains  $\epsilon_1$ ,  $\epsilon_2$ , and  $\epsilon_3$ .

$$(1)$$

$$0 = \begin{vmatrix} \epsilon_x - \epsilon_0 & \epsilon_{xy} & 0 \\ \epsilon_{xy} & \epsilon_y - \epsilon_0 & 0 \\ 0 & 0 & \epsilon_z - \epsilon_0 \end{vmatrix}$$

To facilitate a more accessible comparison between the strains at a particular location, the three principal strains were integrated into a single positive value termed the equivalent strain, shown in (4), based on (2). For this equation the

value of  $\nu'$ , the effective Poisson's ratio, was 0.4.

(2)

$$e_{eq} = \frac{1}{1 + \nu'} \left( \frac{1}{2} [(\epsilon_1 - \epsilon_2)^2 + (\epsilon_2 - \epsilon_3)^2 + (\epsilon_3 - \epsilon_1)^2] \right)^{1/2}$$

After the transformation, the output from each strain gage rosette was plotted against the equivalent strain obtained from the FEA results. From **Figure 5** you can see that there is very good correlation between the theoretical results and the measured results. In the case of the finite element model, this corresponds to a particular nodal location. The nodal location was chosen such that the spatial coordinates best aligned with the actual location of each strain gage rosette with respect to the yoke geometry. To remain concise, only the tail and fillet rosette locations of the yoke are shown in **Figure 6** and **Figure 5**. From knowledge of failed or condemned yokes within the field, and from our proceeding stress analysis it can be seen that the fillet region (strap transition) and the tail section are the two critical locations for failure within a yoke.

In the fillet region where the strap transitions into the butt end the stress can approach critical values exceeding the yield strength of the material and, in some localized areas, the true ultimate strength. Depending on how you define the failure of a material, exceeding either of these values can be

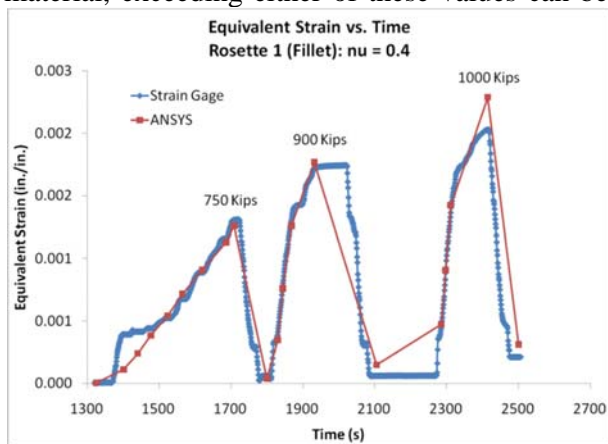


Figure 5: Fillet Rosette Correlation

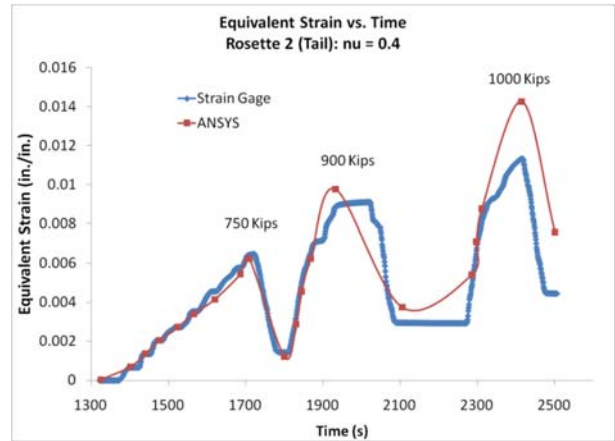


Figure 6: Tail Rosette Correlation

considered a failed component. Since the yoke experiences heavy loading in the field that can cause localized yielding within the material, exceeding the yield strength should not be considered the criterion for failure. To design a yoke to remain elastic for all possible loads would not be practical. Even exceeding the ultimate strength of a material does not necessarily indicate the entire part has fractured, only that a localized crack may occur in the nodal location where the ultimate strength was exceeded. In the fillet region, exceeding the UTS, even in a relatively small region can lead to complete fracture. Since this region has a relatively small cross-sectional area, the initiation of a crack can lead to fracture due to the small distance needed to propagate to complete failure. Assuming that the yoke is manufactured perfectly (no defects, voids, etc.), it takes a very large load to exceed this limit. **Figure 7** shows the fillet region's Maximum Principal Stress at 1000 kips. Near this value of tensile load, complete fracture of a yoke can be considered probable.

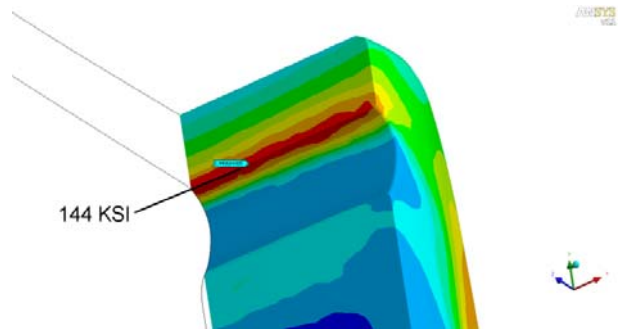


Figure 7: Strap Transition: Maximum Principal Stress

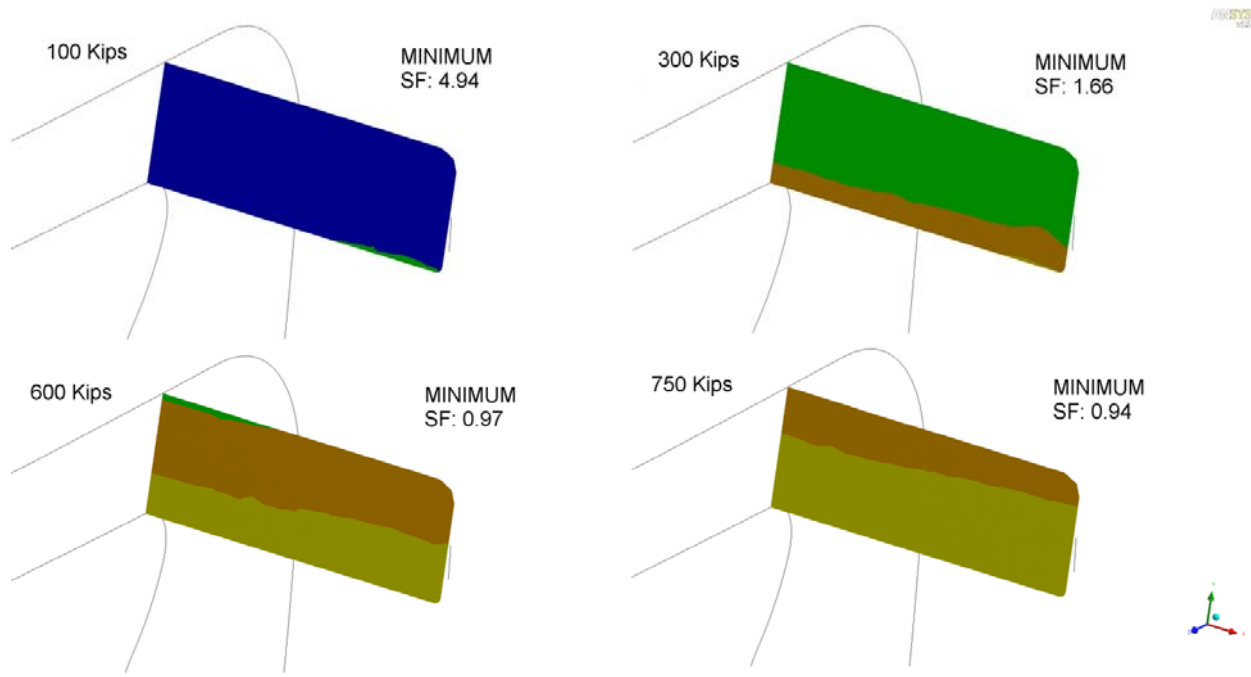


Figure 8: Safety Factor Progression

Viewing the subsequent decrease of the Safety Factor (SF), described in (4), across the cross sectional area of the strap transition region for an increasing tensile load displays the portion of the area approaching the yield limit. **Figure 8** displays this progression, from left to right, as the yoke is loaded to 750 kips. This plot displays the SF at loads of 100, 300, 600 and 750 Kips. If a SF greater than 3 is considered ideal, then a load of 600 Kips will create a stress state where approximately half of the strap cross-sectional area has a SF below this value. In subsequent increase in load further increase the percentage of cross-sectional area below this value.

subject to a large amount of strain. As the load is progressively applied, the tail material is extended around the butt end toward the strap region. This stretching can be illustrated by a plot displaying the maximum principal stress vectors. **Figure 9** displays the tensile vectors (in red) of the tail portion of the yoke under the applied tension.

For the tail portion of the yoke, the material is

As the material is stretched beyond its elastic limit it undergoes permanent nonlinear deformation. This deformation can be represented by a plot of the equivalent plastic strain within the material. **Figure 10** displays a contour plot of the yielded material, with a dark blue color indicating elastic material. This high level of yielding can lead to a weakening of the

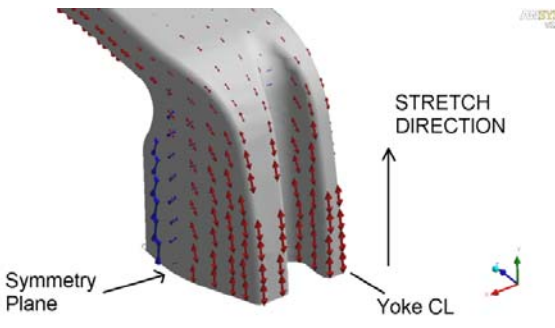


Figure 9: Tail Region Stress Vectors

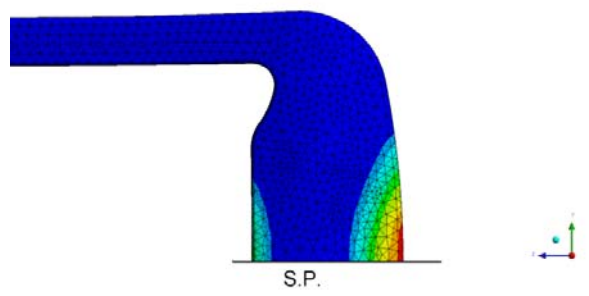


Figure 10: Yielded Material



material in the tail end. After substantial plastic deformation the material can no longer behave in a ductile manner and a crack will initiate within the tail end degrading the yoke's ability to withstand the loading. This degradation of the tail's load carrying capacity can preclude to a fracture in the strap transition region due to the reduced stiffness provided by the cracked tail region. In addition, this excessive deformation of the tail necessitates the bowing inward of the straps thus presenting a situation where binding of the draft gear is a possibility.

### FATIGUE LIFE ASSESSMENT

After developing an understanding of the stress state developed within a yoke during the loading conditions described in M-205, further analysis was performed to gain an insight into the potential fatigue life of a yoke. Assuming that most yoke failure in the field is the product of either accumulated fatigue damage accrued during normal loading cycles or accumulated fatigue damage in conjunction with an abnormally large load, a fatigue analysis was performed. The preliminary fatigue analysis involved the comparison of material parameters on the fatigue life. This analysis was performed using the loading spectrum described in the proposed AAR specification M-216 (5), along with the Modified Goodman Method (MGM) (6). Since the loading in that specification is designed for a knuckle (a theoretically weaker component) and due to potential loading cycles that cause regions of the material to exceed the material yield, some arbitrarily devised loading blocks were created based on the REPOS data available in the AAR Manual (7). Also, since the MGM is a Stress Life fatigue analysis relying on S-N curve data and stresses that remain elastic, a more sophisticated Strain Life fatigue method was used to account for localized plasticity and localized yielding within the material.

For the preceding static stress analysis, the material properties utilized in the FEA program were those obtained from coupon testing of our AAR M-201 Grade E steel (8). That analysis was not intended to illustrate how the material properties will ultimately affect the stress state

developed within a yoke, but only to analyze the critical areas in a general manner. The preliminary Stress Life fatigue analysis required the use of various material curves. Since all of the material parameters used are variations of M-201 Grade E steel, the only pertinent material properties are those describing the plasticity curve that represents the plastic flow of the material after it has exceeded its yield limit. This nonlinear curve can be represented by a power law equation termed the Ramberg-Osgood equation (9) shown in (3) with  $\epsilon_T$  the total strain,  $\sigma$  the stress,  $E$  the elastic modulus,  $K$  the strain hardening coefficient and  $n$  the strain hardening exponent.

$$(3)$$

$$\sigma = K * \left( \epsilon_T - \frac{\sigma}{E} \right)^n$$

Since actual values for  $K$  and  $n$  were not available, a method utilizing the standard material properties (UTS, yield limit, elongation, reduction of area) obtained from a coupon tensile test were used to estimate the strain hardening values as shown in (6). **Figure 11** displays the plasticity curve for each material simulated with the yield limit and the UTS displayed on the chart. The variation in potential UTS from the chemical properties described in M-201 is quite large as can be displayed by the plasticity curves.

Using the loading spectrum described in M-216, all stress values remain below the yield limit in the elastic regime. This allows for the use of the

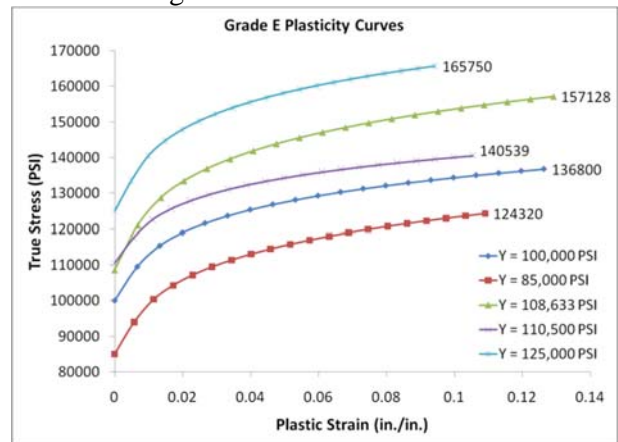


Figure 11: Grade E Plasticity Curves

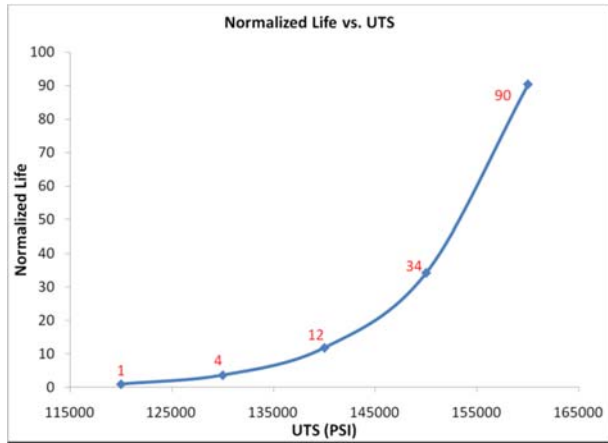


Figure 12: Fatigue Life Increase

MGM to calculate the potential fatigue life of a yoke. After the corresponding stress values are obtained for each load cycle in the spectrum, the MGM is used with (4) to create an equivalent alternating stress ( $S_{eq}$ ) from the alternating stress ( $S_a$ ), the mean stress ( $S_m$ ), and the UTS.

$$(4) \quad S_{eq} = S_a / \left(1 - \frac{S_m}{UTS}\right)$$

S-N curve data is then utilized to calculate the life for each stress cycle. Assuming that the fatigue damage is not sequence dependent, Miner's Rule (6) is then utilized to accumulate the total fatigue damage and the subsequent fatigue life in total cycles.

For this particular fatigue analysis, the UTS of the

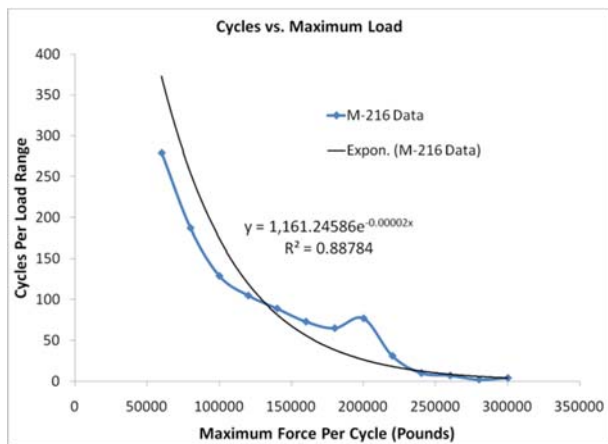


Figure 13: Regression Plot (Loading Spectrum)

yoke material were increased from 120 KSI to 160 KSI. Since fatigue life is a logarithmic correlation, and not a linear one, between stress value and total life, small increases in stress can cause dramatic decreases in potential life. The 33 percent increase in UTS, and its associated yield limit, will have a dramatic increase in the potential life of the yoke. **Figure 12** is a plot of the increase in normalized life as the UTS is increased. The nonlinear nature of the curve is visible and the 33 percent increase in UTS will lead to a 94 times increase in potential life (9400 percent greater life). From the preceding analysis, it can be shown that altering the mechanical properties of the yoke can have a dramatic increase in the potential life. By improving a yoke's UTS (while still maintaining the desired ductility) the potential fatigue life obtained in service can be greatly increased. When performing a Stress Life analysis, it is worth noting that the fatigue life is output as the number of cycles to fracture.

The preceding fatigue analysis performed considered only stress values developed under loading up to a load of 300 kips. This loading spectrum shown in M-216 is not sufficient in accurately predicting the fatigue life of a yoke for the following reasons: M-216 is designed for a theoretically weaker component in the knuckle, the REPOS data displays loads in excess of 300 kips, and freight car mass has been continually increasing over the last 20 years since the original REPOS data was gathered. Using this information, a potential loading spectrum was developed using a regression analysis. To keep this spectrum consistent with M-216, thirteen loading cycles were considered. **Figure 13** displays the general characteristics of the modified loading spectrum where the number of cycles per load range decreases as the load magnitude increases. Assuming that the loading magnitude decreases linearly as the cycles are increased, the regression equation shown in **Figure 13** was utilized to calculate the number of cycles for each loading range.

When analyzing loading cycles where the stress values are exceeding the yield limit, consideration should be made to account for the possible strain hardening or softening of the material during the loading. This material effect is called the Bauschinger Effect (9), and can be incorporated into the pseudo-static FEA analysis by utilizing a cyclic stress-strain curve for the first loading cycle and a hysteresis stress-strain curve for all the subsequent loading cycles (6). When a material strain hardens, an identical strain value will be caused by an increased stress value. The convention for defining the cyclic and the hysteresis curve is similar to that of the Ramberg-Osgood equation (3), and is shown in (6). Utilizing these material laws allows for the modeling of strain-hardening within the Grade E material. A typical hysteresis loop is shown in **Figure 14** representing a plot of stress versus strain for an arbitrary block of Grade E material.

For the Strain Life fatigue analysis, the material parameters utilized were identical to those used in the static stress analysis. When considering a Strain Life fatigue analysis, the state of stress in a particular region determines the method utilized to account for the mean stress effects of a loading cycle. For a purely uniaxial state of stress, the Smith-Watson-Topper (SWT) method was utilized (6). When a surface behaves in a biaxial manner the Brown-Morrow (BM) method was used. A tri-axial stress state is typically not considered as the surface will have no out-of-plane stress value and most cracks initiate on the surface. To determine the particular stress state of a nodal location, the biaxiality indicator (BI) (4) was calculated. The BI is a ratio of the principal stresses with a value of 0 indicating

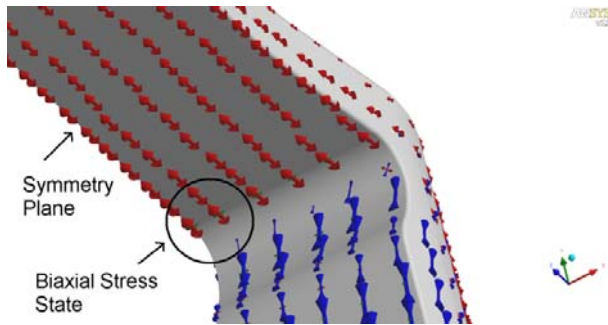


Figure 15: Fillet Region Stress Vectors

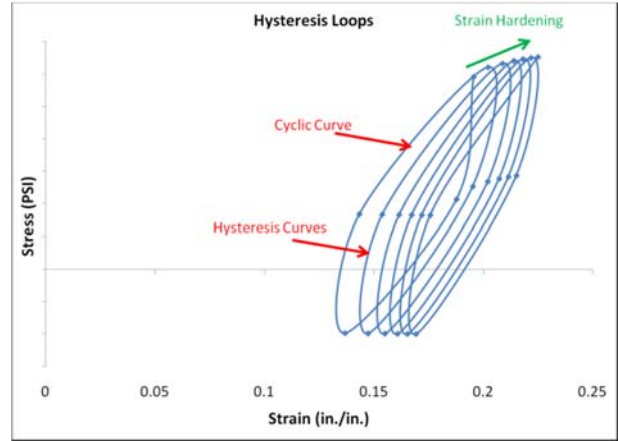


Figure 14: Strain Hardening (Hysteresis)

uniaxial stress, a value of -1 as pure shear, and a value of 1 indicating a purely biaxial stress state. The tail section of the yoke experiences purely tensile stresses approaching a nearly uniaxial state of stress with a BI of approximately zero. From the vector plot shown in **Figure 9** you can see the tensile stress vectors with no contribution from the other principal stresses. Within the fillet radius and strap transition region a more bi-axial stress state is developed, although this region still experiences mainly tensile stresses. From the plot of the maximum principal stress vectors in the fillet region you can visually see the green stress vector indicating that the second principal stress is not negligible in this area. **Figure 15** displays the stress vectors that calculate a biaxiality of 0.22.

Since the tail region was determined to have a uniaxial state of stress, the SWT method was utilized to calculate the potential fatigue life. The SWT method uses the strain range ( $\Delta\varepsilon/2$ ), the maximum stress ( $\sigma_{max}$ ), the elastic modulus ( $E$ ), and the four material constants: fatigue strength coefficient ( $\sigma_f'$ ), fatigue strength exponent ( $b$ ), fatigue ductility coefficient ( $\varepsilon_f'$ ), fatigue ductility exponent ( $c$ ). The SWT fatigue equation is shown in (5).

(5)

$$\frac{\Delta\varepsilon}{2} \sigma_{max} = \frac{(\sigma_f')^2}{E} (2N_f)^{2b} + \sigma_f' \varepsilon_f' (2N_f)^{b+c}$$

**Table 1: Tail Fatigue Life (SWT Method)**

<u>Load Segment</u>	<u>Cycles</u>	<u>Fmax (lbs)</u>	<u>Fmin (lbs)</u>	<u>Strain Range (in./in.)</u>	<u>Smax (PSI)</u>	<u>Life (cycles)</u>
1	7	470000	4700	0.0036	100234	2.E+04
2	9	440000	4700	0.0034	93454	3.E+04
3	13	410000	4700	0.0032	86667	6.E+04
4	18	380000	4700	0.0029	79872	1.E+05
5	28	340000	4700	0.0027	73071	4.E+05
6	38	310000	4700	0.0024	66261	1.E+06
7	53	280000	4700	0.0022	59444	4.E+06
8	74	250000	4700	0.0020	52619	2.E+07
9	103	220000	4700	0.0017	45786	9.E+07
10	144	190000	4700	0.0015	38945	6.E+08
11	200	160000	4700	0.0013	32096	6.E+09
12	278	130000	4700	0.0010	25237	9.E+10
13	431	90000	4700	0.0008	18370	3.E+12
Spectrum Cycles	1396				Total Life	<b>1,191,384</b>
					Repeats	<b>854</b>

Utilizing the FEA results obtained from analyzing the entire loading spectrum described in Figure 13, the fatigue life was calculated for the tail region. Table 1 displays the strain and stress range for each loading segment along with the corresponding life. Table 1 also displays the cumulative damage calculated using Miner's Rule. For the particular loading spectrum used, the total number of cycles for the tail region would be approximately 1.2 million, or 854 repeats of the 1396 cycle loading block.

In contrast to the tail region, the fillet experiences a more biaxial stress state, and the BM method was utilized to calculate the fatigue life of the fillet. This method uses the shear strain range ( $\Delta\gamma/2$ ), normal strain range ( $(\Delta\varepsilon_N)/2$ ), the maximum shear stress ( $\tau_{max}$ ), the maximum normal stress ( $\sigma_{(N,max)}$ ), and the five material constants described in the SWT method. The BM equation is shown in (6).

(6)

$$\begin{aligned} & \frac{\Delta\gamma}{2} \tau_{max} + \frac{\Delta\varepsilon_N}{2} \sigma_{N,max} \\ & = 1.02 \frac{(\sigma'_f)^2}{E} (2N_f)^{2b} \\ & + 1.04 \sigma'_f \varepsilon'_f (2N_f)^{b+c} \end{aligned}$$

In a manner similar to that for the tail region, the fatigue life was calculated for the fillet region. Table 2 summarizes the calculated fatigue life for each loading segment and the corresponding life. Using Miner's Rule to accumulate the fatigue damage, the total life is approximately  $10^9$  cycles, or 1.1 million repeats of the loading block. For this particular application, this value can be considered an infinite life. Based on the two previous analyses, some assumptions can be made regarding the area that will fail first. In a Strain Life fatigue analysis, the fatigue life indicates the initiation of fatigue cracks, not the complete failure of a component. With this understanding, it could be possible for a component to initiate a crack (fatigue life reached) and yet not experience a failure in the field. Assuming that this situation does not occur and that the fatigue crack will rapidly propagate to fracture, it can be shown that the tail portion of the yoke will fail first. This underlies the previous statements that the tail will experience the first minor failure (fatigue cracks) reducing the load carrying capability of the tail end by decreasing the stiffness. With a decreased stiffness in the tail end, the strap transition and the fillet region will experience strains that exceed the maximum values causing a secondary crack to emerge in this area. Since there is very little distance until the complete fracture of a



**Table 2: Fillet Fatigue Life (BM Method)**

<u>Load Segment</u>	<u>Cycles</u>	<u>Force (lbs)</u>		<u>Strain Range (in./in.)</u>		<u>Maximum Stress (PSI)</u>		<u>Life (Cycles)</u>
		<u>Max</u>	<u>Min</u>	<u>Shear</u>	<u>Normal</u>	<u>Shear</u>	<u>Normal</u>	<u>Nf</u>
1	7	470000	4700	0.0028	0.0006	31705	32517	2.E+07
2	9	440000	4700	0.0026	0.0006	29508	30268	4.E+07
3	13	410000	4700	0.0024	0.0005	27331	28040	1.E+08
4	18	380000	4700	0.0022	0.0005	25176	25833	3.E+08
5	28	340000	4700	0.0020	0.0005	23042	23647	8.E+08
6	38	310000	4700	0.0018	0.0004	20931	21484	3.E+09
7	53	280000	4700	0.0016	0.0004	18843	19344	1.E+10
8	74	250000	4700	0.0014	0.0003	16778	17228	4.E+10
9	103	220000	4700	0.0013	0.0003	14739	15136	2.E+11
10	144	190000	4700	0.0011	0.0002	12724	13070	1.E+12
11	200	160000	4700	0.0009	0.0002	10736	11029	1.E+13
12	278	130000	4700	0.0007	0.0002	8774	9016	2.E+14
13	431	90000	4700	0.0006	0.0001	6841	7031	4.E+15
Spectrum Cycles	1396						Total Life	<b>1,530,545,085</b>
							Repeats	<b>1,096,654</b>

strap, the fillet region crack propagates to failure first.

### CONCLUSIONS

Based on test data collected and the analysis done, it was demonstrated that it is possible to accurately determine the stresses and strains in a yoke using FEA software. Having confidence in the correlation between the quasi-static test data and the computer simulations has given the ability to accurately analyze the ultimate strength characteristics of the yoke. The knowledge of the yoke's material response to representative loads allows for the determination of the critical regions. Based on the stress profile developed, it can be determined that the strap transition region (fillet) and the tail region are the most critical. These locations experience high levels of plastic deformation and have maximum stress values that approach the UTS of the material.

In service, the two main failure modes of a yoke are complete fracture and excessive stretching. To improve the performance of a yoke in the field, the material properties can be altered to allow for greater ductility and increased fracture resistance. Increasing the yield and UTS of the Grade E material allows for the yoke to remain in the elastic regime for heavier loads while also

increasing the stress value at which a fracture will occur. If the critical locations of the yoke have enhanced material parameters, the likelihood of a failure can be reduced.

Since a yoke undergoes cyclic loading in the field, fatigue damage must be accounted for in the failure mode of the material. After determining the critical locations within the yoke geometry and calculating their stress profiles, various fatigue methodologies were used to predict the potential life of the fillet region and the tail region.

It is important to consider the type of strain the yoke is experiencing in service in order to properly determine the fatigue life. In localized regions (nodes) of the yoke that experience purely elastic strain, even at relatively high loads, it is most practical to consider a Stress Life fatigue analysis such as the (MGM). However, particular nodes of the yoke geometry will experience plastic strain at high loads thus precluding the use of more sophisticated analysis techniques. This nonlinearity results in hysteresis with the material subsequently strain hardening or softening during the loading cycles. In these nodes and under these loading circumstances, the MGM does not accurately determine the fatigue life of a yoke.

In such instances one must employ a Strain Life fatigue analysis.

Another important factor in accurately determining the fatigue life of a yoke is to know what loading spectrum will accurately represent the loads it will experience while it's in service. There is useful empirical data available for analyzing knuckles, but yokes are purposefully designed to be stronger and to have a longer fatigue life so this data cannot be used without modification. In order to develop a more suitable loading spectrum for the fatigue analysis of a yoke, a regression analysis of the M-216 knuckle loading spectrum was used to develop a heavier loading spectrum that better represents the loads a yoke will experience in service.

For the critical regions (nodes) in the yoke, a determination of the stress state was needed before performing the Strain Life fatigue analysis. The BI was used to describe whether the stress state was uniaxial, biaxial, shear or some combination of these states. Depending on the stress state, a different fatigue analysis technique must be employed to determine an accurate component life. Using a principal stress vector analysis in the FEA simulation, the tail end of the yoke was determined to be in a purely tensile (uniaxial) stress state with a BI of 0. For uniaxial stress states, the SWT method was decided to give the most accurate determination of fatigue damage. In contrast, the relief fillets of the yoke were partially biaxial with a BI of 0.22. This biaxiality determines the use of the BM method for analyzing the fatigue life.

Using each of the aforementioned fatigue calculation methods for the respective nodal locations, in combination with Miner's Rule, the cumulative fatigue life for each of the critical areas on the yoke was determined. For the fillet region, the total life expectancy of the yoke is  $10^9$  cycles, or 1.1 million repeats of the loading block. For this particular analysis, that can be considered infinite life. In contrast, the tail region has a life expectancy of 1.2 millions cycles, or 854 repeats of the loading block. Based on this fatigue analysis it is apparent that the most critical area of the yoke is the tail region.

For a Strain Life analysis, the number of cycles to failure indicates only the initiation of fatigue cracks and not the total fracture of a component. A yoke could develop fatigue cracks and still be serviceable before fracture occurs or before excessive plastic deformation causes the binding of the draft gear. Based on this information, it can be assumed that the tail region will experience the first fatigue cracks causing a reduction in the load carrying capacity of the tail region. With this reduction in stiffness of the tail region, the strap and fillet will experience strains in excess of the material limit, thus causing secondary cracks to form in this region. Since the distance for these cracks to propagate is minimal, the fillet cracks will propagate to fracture of the yoke.

1. **Association of American Railroads.** M-205: Yoke, Coupler - Test Requirements . *AAR Manual of Standards and Recommended Practices.* 2003.
2. **eFunda, Inc.** Strain Rosette for Strain Measurement. *eFunda* . [Online] eFunda, Inc. [http://www.efunda.com/formulae/solid\\_mechanics/mat\\_mechanics/strain\\_gage\\_rosette.cfm](http://www.efunda.com/formulae/solid_mechanics/mat_mechanics/strain_gage_rosette.cfm).
3. **Gere, James M.** *Mechanics of Materials.* s.l. : Brooks/Cole, 2001.
4. **ANSYS, Inc.** *Theory Reference for ANSYS and ANSYS Workbench.* [Documentation] s.l. : ANSYS, Inc., 2007.
5. **Association of American Railroads.** M-216: Knuckle, Types E and F - Fatigue Test. *AAR Manual of Standards and Recommended Practices.* 2009.
6. **Draper, John.** *Modern Metal Fatigue Analysis.* s.l. : Safe Technology Limited, 2004.
7. **Association of American Railroads.** M-1001, Chapter 7: Fatigue Design of New Freight Cars. *AAR Manual of Standards and Recommended Practices.*
8. —. M-201: Castings, Steel. *AAR Manual of Standards and Recommended Practices.* 2005.
9. **ASM.** *Atlas of Stress-Strain Curves.* 2002.